[11] G. Lanarque, C. Viton, A. Domard, *Biomacromol.* **2004**, *5*, 1899.
[12] S. C. Tan, E. Khor, T. K. Tan, S. M. Wong, *Talanta* **1998**, *45*, 713.
[13] S. Yagi, D. Kunii, *Chem. Eng. Sci.* **1961**, *16*, 364.
[14] O. Levenspiel, *Chemical Reaction Engineering*, 2nd ed., John Wiley & Sons, Inc., New York **1972**.
[15] K. Kurita, T. Sannan, Y. Iwakura, *Makromol. Chem.* **1977**, *178*, 3197.
[16] Y. M. Dong, Y. H. Ruan, Y. S. Wu, *Chem. Res. Chin. Univ.* **2000**, *23 (3)*, 490.

MD Simulations of Diffusivities in Methanol-n-hexane Mixtures Near the Liquid-liquid Phase Splitting Region

By *R. Krishna** and *J. M. van Baten*

DOI: 10.1002/ceat.200500376

Molecular Dynamics (MD) simulations have been carried out to determine the self-diffusivities in binary mixtures of methanol and n-hexane with varying compositions at four different temperatures of 303.15 K, 307.7 K, 310.7 K, and 313.15 K. The Darken relation was used to determine both the Fick diffusivity and the Maxwell-Stefan diffusivity. The values of the Fick diffusivity obtained from the simulations are in very good agreement with published experimental data of Clark and Rowley [17]. These diffusivities approach zero near composition regions where liquid-liquid phase splitting occurs. On the other hand, the Maxwell-Stefan diffusivity is well-behaved and appears to be practically insensitive to the complex thermodynamics.

1 Introduction

The Maxwell-Stefan (M-S) Eqs. (1–3) are gaining widespread usage in describing diffusion in bulk fluids and in porous materials. For binary diffusion the M-S equation is [1]:

$$-\frac{1}{RT}\nabla\mu_1 = \frac{x_2(\mathbf{u}_1 - \mathbf{u}_2)}{Đ_{12}} \tag{1}$$

In Eq. (1), $\mathbf{u}_i$ is the ensemble-averaged velocity of species i, x_i is the mole fraction of species i, and $Đ_{12}$ is the M-S diffusivity. There is only one independent driving force because of the Gibbs-Duhem relationship:

$$x_1\nabla\mu_1 + x_2\nabla\mu_2 = 0 \tag{2}$$

The molar average reference velocity $\mathbf{u}$ is:

$$\mathbf{u} = x_1\mathbf{u}_1 + x_2\mathbf{u}_2 \tag{3}$$

The diffusion fluxes of component i, $\mathbf{J}_i$, with respect to the molar average reference velocity $\mathbf{u}$ are defined by:

$$\mathbf{J}_i = c_t x_i(\mathbf{u}_i - \mathbf{u}),\ i = 1, 2 \tag{4}$$

For a binary mixture the Fick diffusivity D_{12} is defined by:

$$\mathbf{J}_1 = -c_t D_{12}\nabla x_1 = -\mathbf{J}_2 = c_t D_{12}\nabla x_2 \tag{5}$$

and equals the M-S diffusivity multiplied by the thermodynamic correction factor Γ:

$$\mathrm{D}_{12} \equiv Đ_{12}\Gamma = Đ_{12}\left(1 + \frac{\partial \ln\gamma_1}{\partial \ln x_1}\right) \tag{6}$$

where γ_1 is the activity coefficient of component 1.

The Darken relation [4] postulates that the composition dependence of the Fick diffusivity D_{12} is given by:

$$\mathrm{D}_{12} = \left(x_2\mathrm{D}_{1,\mathrm{self}} + x_1\mathrm{D}_{2,\mathrm{self}}\right)\left(1 + \frac{\partial \ln\gamma_1}{\partial \ln x_1}\right) \tag{7}$$

where $D_{1,\mathrm{self}}$ and $D_{2,\mathrm{self}}$ are tracer, or self-diffusivities of components 1 and 2 in the mixture. Combining Eqs. (6) and (7) the following expression for the composition dependence of the M-S diffusivity $Đ_{12}$ in a *binary* mixture is obtained:

$$Đ_{12} = x_2\mathrm{D}_{1,\mathrm{self}} + x_1\mathrm{D}_{2,\mathrm{self}} \tag{8}$$

The $D_{1,\mathrm{self}}$ and $D_{2,\mathrm{self}}$ are more easily accessible, both experimentally [5–7] and from Molecular Dynamics (MD) simulations [8–16], than the $Đ_{12}$. Recent work [16] has confirmed the applicability of Eq. (8) for mixtures of linear alkanes.

The thermodynamic factor Γ approaches zero for temperatures and compositions for which liquid-liquid phase splitting can occur [17, 18]. Consequently, the Fick diffusivity D_{12} also tends to approach vanishingly small values. This has been confirmed experimentally by Clark and Rowley [17] for diffusion in methanol-n-hexane mixtures. It has always been claimed in the literature that the M-S diffusivity $Đ_{12}$ is well-behaved, displaying no severe composition dependences. The major objective of the present communication is to examine the extent to which the experimental data of Clark and Rowley can be confirmed by MD simulations. In particular the accuracy of the Darken relation (Eq. (8)) is examined for an estimation of the Fick diffusivity.

2 MD Simulations

The details of the MD simulation technique to determine self diffusivities in pure component and *binary* mixtures are well-documented in the literature [8–16]. The presented im-

[*] R. Krishna (author to whom correspondence should be addressed, r.krishna@uva.nl), J. M. van Baten, Van`t Hoff Institute for Molecular Sciences, University of Amsterdam, Nieuwe Achtergracht 166, 1018 WV Amsterdam, The Netherlands.

1) List of symbols at the end of the paper.

plementation uses the DL_POLY_2 code [19] and the simulation details are essentially the same as the ones reported in an earlier publication [16]. For methanol, we use the three-site (CH_3, O, H) united atom approach combining Lennard-Jones and Coulombic interactions; the parameter values are taken from Van Leeuwen and Smit [20]. For n-hexane the united atom model is also employed and the CH_x groups are considered as single, chargeless interaction centers with their own effective potentials. The beads in the chain are connected by harmonic bonding potentials. A harmonic cosine bending potential models the bond bending between three neighboring beads, a Ryckaert-Bellemans potential controls the torsion angle. The beads in a chain separated by more than three bonds interact with each other through a Lennard-Jones potential. The Lennard-Jones potentials are shifted and cut at 12 Å. The force fields for n-alkanes have been given in detail in other publications [21]. The Lorentz-Berthelot mixing rules have been used to describe inter-molecular Lennard-Jones interaction parameters.

A minimum of $N = 100$ molecules was used and the size of the simulation box was adjusted on the basis of the estimated mixture densities from the data in [17, 18]. This yields simulation box sizes varying from 25 Å to 28 Å, depending on the mixture composition. For example, for the temperature of 313.15 K the molecular loading and box sizes were (a) $x_1 = 0.05$, $N = 100$, box size = 27.61345 Å, (b) $x_1 = 0.5$, $N = 120$, box size = 25.73282 Å, and (c) $x_1 = 0.9$, $N = 200$, box size = 25.42906 Å. Periodic boundary conditions were employed.

The self-diffusivities were determined from the formula:

$$D_{i,self} = \frac{1}{6N_i} \lim_{\Delta t \to \infty} \frac{1}{\Delta t} \left\langle \left(\sum_{l=1}^{N_i} \left(r_{l,i}(t + \Delta t) - r_{l,i}(t) \right)^2 \right) \right\rangle \qquad (9)$$

where $\mathbf{r}_{l,i}(t)$ denotes the position vector of molecule l of species i, N_i is the number of molecules of species i, and the notation $\langle \cdots \rangle$ denotes ensemble averaging.

The simulations were carried out on clusters of PCs equipped with Intel Xeon processors running at 3.4 GHz on the Linux operating system. Each simulation campaign run was run for a period of 48 h; this was sufficient to obtain reliable statistics for the determination of the diffusivities.

3 Simulation Results and Discussion

Fig. 1 shows the simulation data of the self-diffusivities $D_{i,self}$ at (a) 313.15 K and (b) 310.7 K, along with the M-S diffusivity $Đ_{12}$ calculated using the Darken relation (Eq. (8)). Using the NRTL activity coefficient model, the thermodynamic factor Γ can be calculated with the parameters given by Clark and Rowley [17]. The Fick diffusivity D_{12} was then calculated using Eq. (7); these values are compared with the experimental D_{12} data in Fig. 2 for temperatures of (a) 313.15 K, (b) 310.7 K, (c) 307.7 K, and (d) 303.15 K. At the highest two temperatures of 313.15 K and 310.7 K the system forms a homogeneous liquid phase for the entire composition range. For the lower temperatures of 307.7 K and 303.15 K liquid-liquid phase splitting takes place for a range of liquid compositions. The agreement between the MD simulations and experimental data is very good for all four temperatures. The sharp decrease in the Fick diffusivity as the mixture composition approaches that corresponding to phase splitting is reflected correctly in the simulations in all cases. In contrast to the severe composition dependence of the Fick diffusivity, the M-S diffusivity $Đ_{12}$ shows only a mild dependence on mixture composition (s. Fig. 1).

The results presented in Fig. 2 underline the validity of the Darken relation (Eq. (7)) for the estimation of the Fick diffusivity D_{12} from information on the self-diffusivities in the mixture.

4 Conclusions

By performing MD simulations the applicability of the Darken relation (Eq. (7)) for estimation of the Fick diffusivity D_{12} for binary mixtures of methanol-n-hexane at four different temperatures has been verified. From a practical

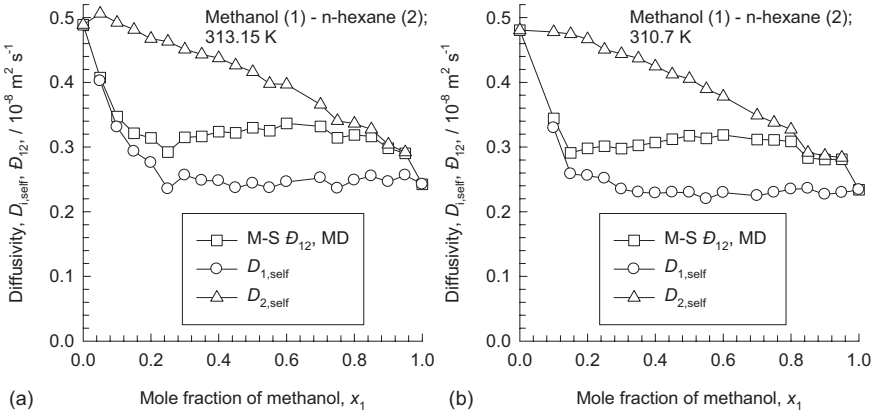

Figure 1. MD simulation results for self-diffusivities, $D_{i,self}$, along with the M-S diffusivities, $Đ_{12}$, calculated from the Darken relation (Eq. (8)) for methanol-n-hexane mixtures at (a) 313.15 K and (b) 310.7 K.

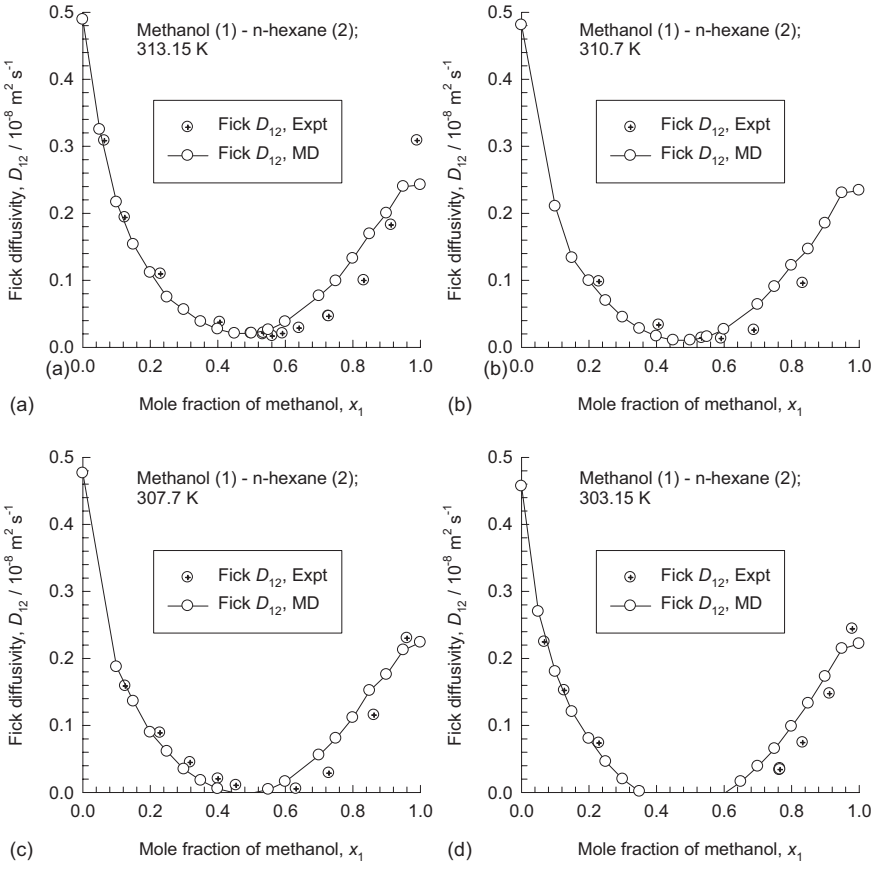

Figure 2. MD simulation results for the Fick diffusivities, D_{12}, calculated from the Darken relation (Eq. (7)), for methanol-n-hexane mixtures at (a) 313.15 K, (b) 310.7 K, (c) 307.7 K, and (d) 303.15 K. Also shown are the experimental data of Clark and Rowley [17].

viewpoint, it is necessary to develop correlations for the self-diffusivites $D_{i,self}$ in mixtures that will allow the prediction of the Maxwell-Stefan $Đ_{12}$ and the Fick diffusivity D_{12}.

Acknowledgements

RK acknowledges the receipt of a TOP subsidy from the Netherlands Foundation for Fundamental Research (NWO-CW) for intensification of reactors. We acknowledge NWO/NCF for provision of high performance computing resources in terms of PC clusters.

Received: November 20, 2005

Symbols used

c_t	[mol m^{-3}]	total molar concentration
$D_{i,self}$	[m^{2}s^{-1}]	self-diffusivity
D_{12}	[m^{2}s^{-1}]	Fick diffusivity in a binary mixture
$Đ_{12}$	[m^{2}s^{-1}]	Maxwell-Stefan diffusivity
N_i	[–]	number of molecules of species *i* in the simulation box
N	[–]	total number of molecules in the simulation box
R	[J mol^{-1}K^{-1}]	gas constant
t	[s]	time
$\mathbf{u}$	[m s^{-1}]	molar average mixture velocity
$\mathbf{u}_i$	[m s^{-1}]	ensemble-averaged velocity of species *i*
x_i	[–]	mole fraction of species *i*
T	[K]	absolute temperature

Greek letters

Γ	[–]	thermodynamic factor
γ_i	[–]	activity coefficient of species *i*
μ_i	[J mol^{-1}]	molar chemical potential

References

[1] R. Krishna, J. A. Wesselingh, *Chem. Eng. Sci.* **1997**, *52*, 861.
[2] R. Taylor, R. Krishna, *Multicomponent Mass Transfer*, John Wiley & Sons, Inc., New York **1993**.
[3] J. A. Wesselingh, R. Krishna, *Mass Transfer in Multicomponent Mixtures*, VSSD, Delft, The Netherlands **2000**.
[4] L. S. Darken, *Trans. Inst. Min. Metall. Engrs.* **1948**, *175*, 184.

[5] J. C. Shieh, P. A. Lyons, *J. Phys. Chem.* **1969**, *73*, 3258.
[6] D. L. Bidlack, D. K. Anderson, *J. Phys. Chem.* **1964**, *68*, 206.
[7] M. Helbaek, B. Hafskjold, D. K. Dysthe, G. H. Sorland, *J. Chem. Eng. Data* **1996**, *41*, 598.
[8] D. J. Keffer, P. Adhangale, *Chem. Eng. J.* **2004**, *100*, 51.
[9] G. A. Fernandez, J. Vrabec, H. Hasse, *Int. J. Thermophys.* **2004**, *25*, 175.
[10] T. Merzliak, A. Pfennig, *Mol. Simul.* **2004**, *30*, 459.
[11] G. H. Goo, G. H. Sung, S. H. Lee, T. Y. Chang, *Bull. Korean Chem. Soc.* **2002**, *23*, 1595.
[12] K. P. Travis, D. Brown, J. H. R. Clarke, *J. Chem. Phys.* **1995**, *102*, 2174.
[13] V. A. Harmandaris, D. Angelopoulou, V. G. Mavrantzas, D. N. Theodorou, *J. Chem. Phys.* **2002**, *116*, 7656.
[14] I. M. J. J. Van de Ven-Lucassen, T. J. H. Vlugt, A. J. J. Van der Zanden, P. J. A. M. Kerkhof, *Mol. Phys.* **1998**, *94*, 495.
[15] D. Frenkel, B. Smit, *Understanding Molecular Simulations: From Algorithms to Applications*, Academic Press, San Diego, CA **2002**.
[16] R. Krishna, J. M. Van Baten, *Ind. Eng. Chem. Res.* **2005**, *44*, 6939.
[17] W. M. Clark, R. L. Rowley, *AIChE J.* **1986**, *32*, 1125.
[18] M. Pertler, E. Blass, G. W. Stevens, *AIChE J.* **1986**, *42*, 910.
[19] W. Smith, M. Leslie, T. R. Forester, TheDL_POLY_2 user manual, http://www.cse.clrc.ac.uk/msi/software/DL_POLY/MANUALS/USRMAN2/USRMAN.html, **2005**.
[20] M. E. Van Leeuwen, B. Smit, *J. Phys. Chem.* **1995**, *99*, 1831.
[21] D. Dubbeldam, S. Calero, T. J. H. Vlugt, R. Krishna, T. L. M. Maesen, B. Smit, *J. Phys. Chem. B* **2004**, *108*, 12301.

Preparation and Characterization of a Solid Acid Catalyst from Commercial Niobia Hydrate

By *Benjamin Frank*, *Alparslan Yildiz*, *Daniela Habel*, *Helmut Schubert*, and *Reinhard Schomäcker*

DOI: 10.1002/ceat.200500380

A commercially available niobia hydrate, which is an industrial intermediate in the production of pure niobia, was prepared, characterized, and tested as a solid acid catalyst. The gas phase esterification of acetic acid with ethanol was used as a simple model reaction for the determination of the acidity and the catalytic activity. The kinetic evaluation of the experiments includes an estimation of mass transport limitation as well as a mechanistic study.

1 Introduction

The use of solid acids instead of liquid mineral acids for catalytic applications is characterized by higher process stability and being environmentally less harmful, as well as being less dangerous processes. Niobic acid, a water-containing niobia, has proved to be a suitable catalyst for several reactions [1–4]. Especially for acid catalyzed reactions with water as a reactant or reaction product, niobic acid keeps a high activity, whereas other solid acids partly lose their activity in contact with water or steam. Thus, niobic acid can be used as a catalyst in several reactions [4]. In our experimental studies we could observe catalytic activity for the following reactions: oxidative dehydrogenation of propane, esterification of acetic acid with ethanol and 2-propanol, *N*-alkylation of aniline with ethanol, and dehydration of 2-propanol. The esterification was chosen as a model reaction for the characterization of the catalyst, since side reactions, etherification and dehydration of ethanol, were shown to appear only at high temperatures and can be neglected in the chosen temperature range of 150–220 °C [5]. This is a great simplification for conversion measurement and development of kinetic models.

Our previous research focused on the *N*-alkylation of aniline with ethanol [6, 7] over an industrial niobic acid catalyst. By means of a kinetic study we could show that the reaction pathway occurs via an adsorbed ethoxy species. The observed kinetics agreed well with the Eley/Rideal mechanism. From these results we suggested adsorbed ethanol as the transition state to be attacked by aniline out of the gas phase. One aim of this study was to investigate similarities between *N*-alkylation and esterification concerning the ethoxy group as the transition state. Several studies on the heterogenously catalyzed esterification of acetic acid with ethanol revealed inconsistent theories concerning the microkinetics. Besides the mainly postulated Langmuir/Hinshelwood mechanism (LH) [8–11], Eley-Rideal kinetics with ethanol as the adsorbed species was also found in the literature [8–12]. A change in the mechanism from LH to ER (dual-site to single site) depending on the chain length of the alcohols (short to long chain) was also proposed [13]. Since alcohols adsorb more strongly on the catalyst surface, this theory was explained by sterical hinderance of the adsorption of carboxylic acid by the long alkyl chains of the alcohol. A second explanation could also be a greater influence of the catalyst itself on the reaction pathway, since the studies were carried out over ion-exchange resins, zeolites, or other solid acids.

Another question for our experimental program was the suitability of a commercial niobia hydrate as a catalyst precursor. The influence of the pelletizing pressure, as well as particle size and the modification of the catalytic activity by treatment with phosphoric and sulfuric acid were tested.

2 Experimental

The catalytic measurements were carried out in a stainless steel tubular reactor (l = 130 mm, d = 10 mm), which was heated by a surrounding aluminum block with six cartridge heaters (each 120 W). The pelletized catalyst, usually 1.0 g,

[*] Dipl.-Ing. B. Frank, Dipl.-Ing. A. Yildiz, Prof. Dr. rer. nat. R. Schomäcker (author to whom correspondence should be addressed, schomaecker@tu-berlin.de), Technical University of Berlin, Institute of Chemistry, Straße des 17. Juni 124, D-10623 Berlin, Germany; Dipl.-Ing. D. Habel, Prof. Dr. rer. nat. H. Schubert, Technical University of Berlin, Institute of Material Sciences and Technologies, Englische Straße 20, D-10587 Berlin, Germany.

